

Full Length Research Paper

Automated optical inspection system for analogical resistance type touch panel

Yen-Chung Chen*, Jiun-Hung Yu, Mu-ChiauXie and Fang-Jung Shiou

Opto-mechatronics Technology Center, National Taiwan University of Science and Technology, Taipei 10607, Taiwan.

Accepted 30 May, 2011

The touch panel is the most important and promising technical product nowadays. Automated optical inspection (AOI) technology provides objective measurement, shorter production period and better production quality. The purpose of this paper is to develop an automated optical inspection system for analogical resistance type touch panel. This system integrates mechanism, electrical control and machine vision, and applies digital image processing method, such as Fourier transform, edge detection, thresholding, morphology, particle analysis, etc., to inspect defect of the type touch panel. Finally, the experimental results from touch panel samples show that the automated inspection system can detect and classify defects efficiently.

Key words: Fourier transform, touch panel, automated optical inspection (AOI), image processing.

INTRODUCTION

Touch panel is a common device which can be utilized as human interface in numerous technical products, such as smart phone, ATM, portable media player, etc. The inspection of view-area of touch panel is needed for maintaining touch panel quality. Figure 1 shows the picture of touch panel. Figure 2 shows the illustration of touch panel. Some typical defects including linear foreign matter, scratch and spot, will appear in the view-area as shown in Figure 3. So far, the defects of touch panel have been inspected by human inspectors using electronic microscopes. However, the human inspectors have a disadvantage, that is, they are prone to weariness caused by long-term working. Moreover, some spot defects, which shapes are similar to the dot spacer, are difficult to be detected by human. Therefore, in order to decrease the cost of the inspection process and to increase the competitive advantage of the touch panel, we propose an automated optical inspection (AOI) system to inspect touch panel defects.

Currently, there are no reports on the inspection of touch panel defects using the AOI system. However, we have found some related studies for the inspection of the

textual surface. Some studies to detect defects in directional textured surfaces usually start with a forward transform and filtering, followed by an inverse transform and thresholding (Kumar, 2008). Then, only the defects were preserved in the original image and all the directional textures were removed. These studies applied discrete Fourier transform (Escofet et al., 1998; Tsai and Hsieh, 1999; Chan and Pang, 2000; Perng et al., 2010), discrete wavelet transform (Tsai and Chiang, 2003), singular value decomposition (Lu and Tsai, 2005), independent component analysis (Lu and Tsai, 2008), non-negative matrix factorization (Perng et al., 2008) and principal component analysis (Chen and Perng, 2011) to detect surface defects. Each of these methods was suitable for inspection of directional textured surfaces, because these methods require neither textural features nor any reference image for comparison, they are not confined by the limitations of feature extraction based methods or golden template matching methods (Lin and Ho, 2007). Moreover, commercial AOI products (made by UTECHZONE CO) are provided for the touch panel indium tin oxide (ITO) glass inspection (UTECHZONE, 2009).

In this paper, the proposed AOI system comprises mechanism, electrical control and inspection methods based on Fourier transformation and morphological operation. Owing to a faultless view-area of touch panel

*Corresponding author. E-mail: aron1229@gmail.com. Tel: +886-2-27301297. Fax: +886-2-27301143.

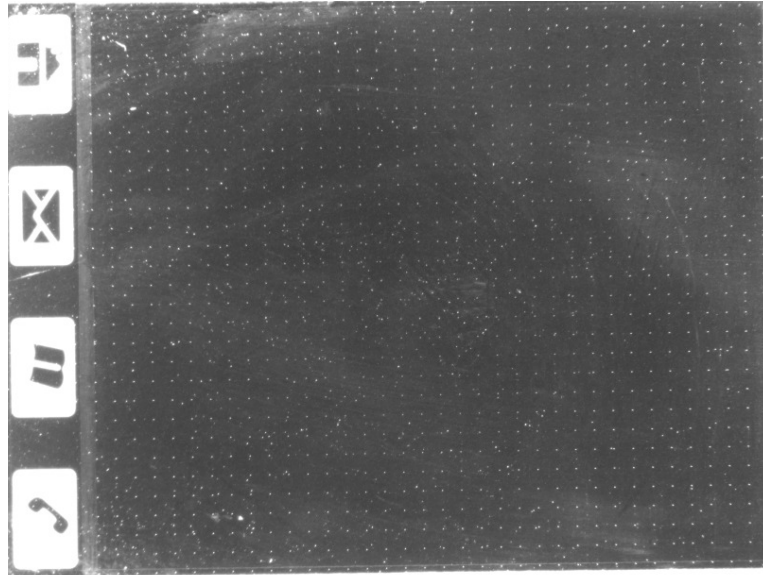


Figure 1. The picture of a touch panel.

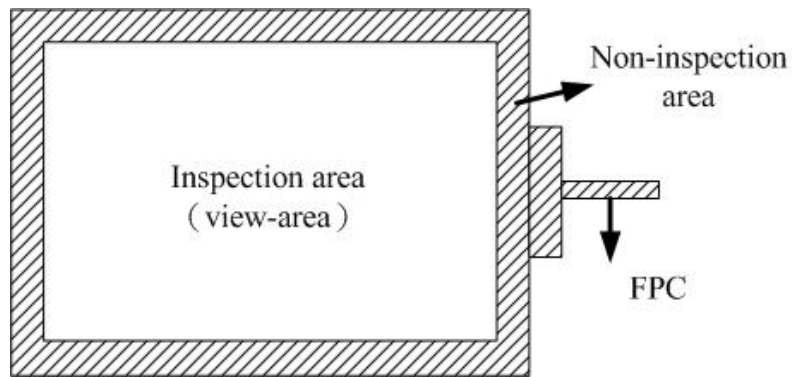


Figure 2. The illustration of a touch panel.

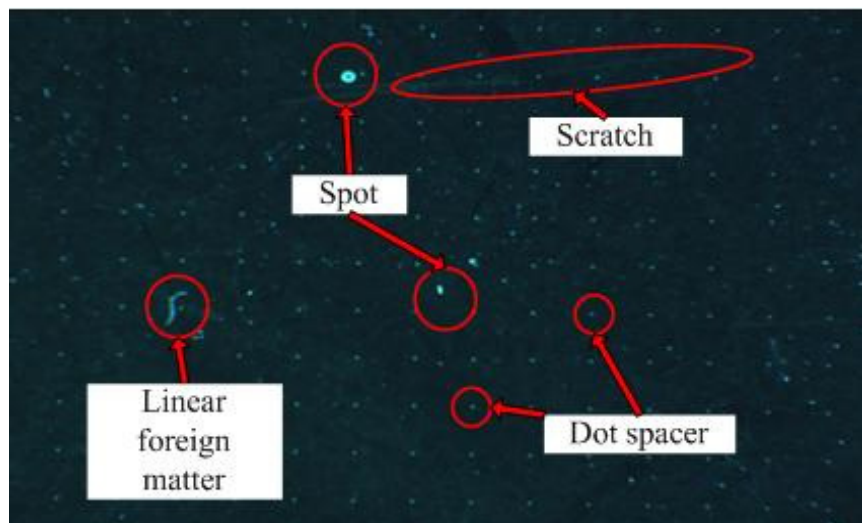


Figure 3. Types of defects on the view-area of touch panel.

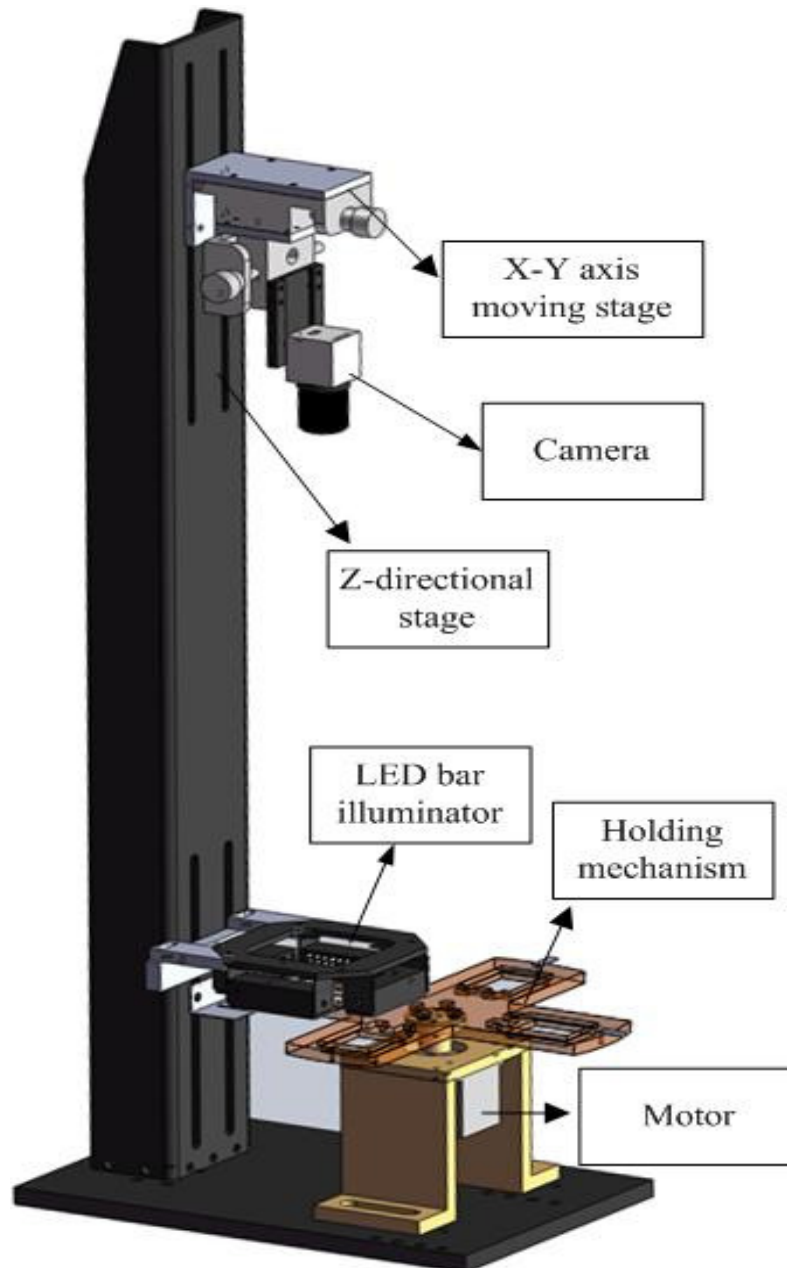


Figure 4. The illustration of hardware of the proposed AOI system.

has a periodic and regular structure; the defects of view-area would be detected easily by Fourier transformation. The proposed AOI system would also perform defect classification.

MATERIALS AND METHODS

AOI system for touch panel inspection

The hardware of the proposed AOI system includes moving stages, CMOS camera, LED bar illuminator and a holding mechanism. The LED bar illuminator is used to illuminate the defects and spacers of

view-area. The single-axis stage provides the z-directional rotation to convey the inspected touch panels. A z-directional stage and X-Y axis moving stage are used for fine-tuning of the position of camera manually to capture clear images. The holding mechanism is used to hold the touch panel during the whole inspecting procedure. The detailed setup of the hardware is shown in Figure 4. The holding mechanism driven by a motor was employed to provide the rotation to convey the inspected touch panels. Figure 5 shows the overall functional block diagram of the proposed AOI system. The whole system was functional divided into mechatronics subsystem module and image grabbing subsystem module. Both modules were commanded from a host personal computer (PC). In the mechatronics subsystem module, a national instruments PCI-7344 four-axis motion control card was national instruments PCI-7344

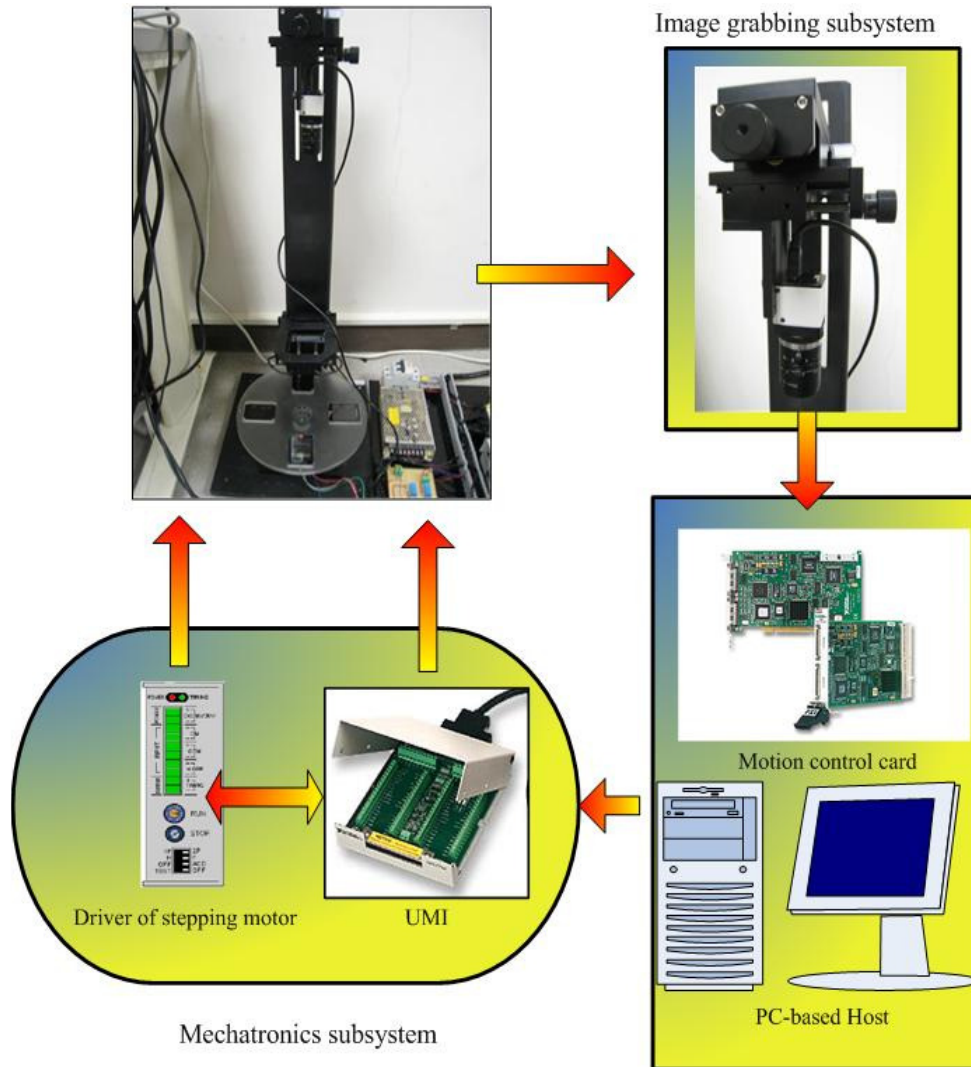


Figure 5. Overall functional block diagram of the proposed AOI system.

four-axis motion control card was installed in the host PC to manipulate the stepping motor. The Troy PK564-B five-phase stepping motor was driven through a Troy TR515B five-phase driver which achieved an angular resolution of 0.72° . In image grabbing subsystem module, an ALTAIR U500 USB camera with 5 million pixels and a Sakai 35 mm focal length CCTV lens were adopted, which achieved an image resolution of $18.45 \mu\text{m}/\text{pixel}$. A LED bar illuminator with a length of 100 mm is adopted to provide stable illumination with small incident angle on the touch panel.

For the purpose of inspection of touch panel, the touch panel is placed on the holding mechanism. The LED bar illuminator highlights not only defects, but also dot spacers. Then, an image of view-area of touch panel can be grabbed by utilizing the CMOS camera. The grabbed image of faultless view-area has a periodic regular global structure which is formed by dot spacers. The occurrence of a defect in the view-area means the regular structure has been destroyed. The Fourier spectrum (Gonzalez and Woods, 2002) is ideally suited for describing the periodic structure in the gray-level images. Hence, in this paper we propose a method based on two-dimensional (2D) Fourier transform (FT) for identifying the defects in the viewing area of touch panel.

The periodic characters of a gray-level image clearly correspond

to high-energy frequency components. The frequency components of the periodic structure in the Fourier domain image are detected by a pre-specified mask, then eliminated by setting them zero. After clearing the specific regions, we back-transform the Fourier domain image using the inverse Fourier transform (IFT). The IFT process will remove all periodic structures in the original gray-level image, and preserves only local anomalies, that is, defects, if they appear in the view-area. A threshold is determined for distinguishing between defects and homogeneous regions in the restored image. Finally, morphological method and shape analysis method (Costa and Cesar, 2000) are applied to classify the defects according to shape features of defects. The overall diagram is shown in Figure 6.

Fourier transform

The FT characterizes the view-area image in terms of frequency components. The periodically occurring features, such as structural dots can be observed from magnitude of frequency components. Such periodic regular global structure is easily distinguishable as concentration of high-energy bursts in spectrum. The discrete 1D FT of $f(x)$ is given by:

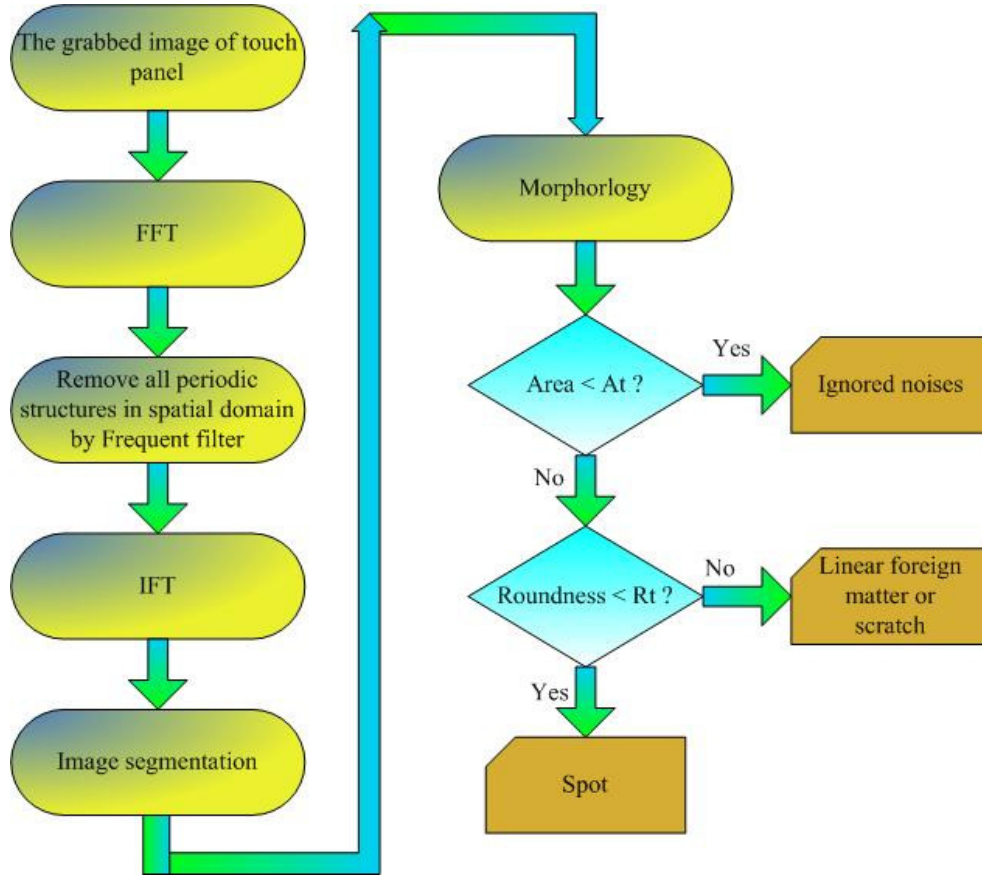


Figure 6. The overall diagram of inspection method (At and Rt which are experimental determined threshold are used to classify defects).

$$F(u) = \frac{1}{M} \sum_{x=-\frac{M}{2}}^{\frac{M}{2}} f(x) \cdot \exp[-j \cdot 2\pi(ux/M)] \quad (1)$$

for frequency variables $u = -\frac{M}{2}, \dots, \frac{M}{2}$.

Let $f(x, y)$ be the gray level at (x, y) in the original image of size $M \times N$. The discrete 2D FT of $f(x, y)$ is given by:

$$F(u, v) = \frac{1}{MN} \sum_{x=-\frac{M}{2}}^{\frac{M}{2}} \sum_{y=-\frac{N}{2}}^{\frac{N}{2}} f(x, y) \cdot \exp[-j \cdot 2\pi(ux/M + vy/N)] \quad (2)$$

for frequency variables $u = -\frac{M}{2}, \dots, \frac{M}{2}$, $v = -\frac{N}{2}, \dots, \frac{N}{2}$.

The FT is generally complex; that is:

$$F(u, v) = R(u, v) + j \cdot I(u, v)$$

where $R(u, v)$ and $I(u, v)$ are the real and imaginary components of $F(u, v)$, that is:

$$R(u, v) = \frac{1}{\sqrt{MN}} \sum_{x=-\frac{M}{2}}^{\frac{M}{2}} \sum_{y=-\frac{N}{2}}^{\frac{N}{2}} f(x, y) \cdot \cos[2\pi(ux/M + vy/N)] \quad (3)$$

$$I(u, v) = \frac{1}{\sqrt{MN}} \sum_{x=-\frac{M}{2}}^{\frac{M}{2}} \sum_{y=-\frac{N}{2}}^{\frac{N}{2}} f(x, y) \cdot \sin[2\pi(ux/M + vy/N)] \quad (4)$$

The power spectrum $P(u, v)$ of $f(x, y)$ is defined by:

$$P(u, v) = |F(u, v)|^2 = R^2(u, v) + I^2(u, v) \quad (5)$$

The 1D FT is used to demonstrate the response of regular structure of dots in Fourier spectrum. Artificial images (128 × 1 pixels) with the regular spacing of 16 pixels are shown in Figure 7a. The corresponding Fourier spectrum is shown in Figure 7b. It reveals that the peaks will appear symmetrically and regularly around the center of Fourier spectrum. The distance (frequency) between two adjacent peaks is fixed. Note that the distance between two

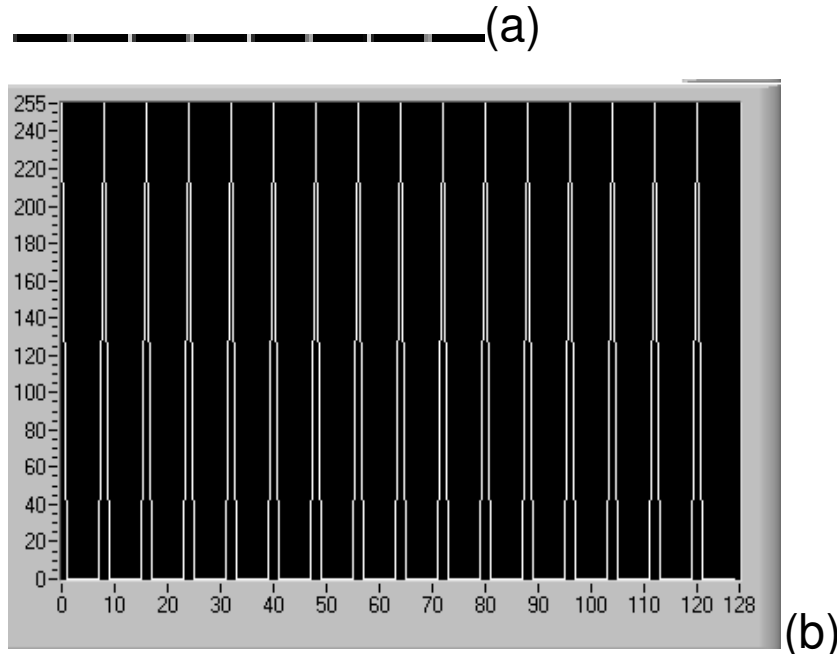


Figure 7. 1D artificial periodic image and corresponding Fourier spectrum: (a) artificial periodic image with wavelength of 16 pixels (b) the corresponding Fourier Spectrum of (a) (distance between two adjacent peaks is 8 pixels).

adjacent peaks in Fourier spectrum relates to the frequency of the periodic dots in the artificial images. The relation between the wavelength of periodic dots in the spatial image and the distance between two adjacent peaks in the Fourier spectrum is given by:

$$\Delta u = M \times \frac{1}{\Delta x} \tag{6}$$

where M is the width of the 1D image, Δx is the wavelength of periodic dots in the spatial image, Δu is the distance between two adjacent peaks in the Fourier spectrum. This feature can be extended to 2D FT and utilized to design the mask to remove the periodic dots structure of the view-area of touch panel.

The horizontal and vertical distance between two adjacent spacers is noted as Δx and Δy , respectively as shown in Figure 8a. The Fourier spectrum of a touch panel is given in Figure 8b. It shows that the periodic spacers in spatial domain image result in periodic dots, and some defects generate multiple diffuse points around central component in Fourier spectrum. Δu and Δv represents the horizontal and vertical distance between two adjacent peaks. Once we get the Δx and Δy , the Δu and Δv will be derived by Equation 7.

$$\Delta u = M \times \frac{1}{\Delta x} , \Delta v = N \times \frac{1}{\Delta y} \tag{7}$$

When the Δu and Δv are obtained, the mask will be generated by Equation 8.

$$F(u, v) = 0 \text{ for all } u, \text{ and } |v| \leq \left[\frac{w}{2} \right] \tag{8}$$

$$F(u, v) = 0 \text{ for all } v, \text{ and } |u| \leq \left[\frac{w}{2} \right]$$

$$F(u, v) = 0 \text{ if } \left| |u| - i \times \Delta u \right| \leq \left[\frac{w}{2} \right], \text{ and}$$

$$\left| |v| - j \times \Delta v \right| \leq \left[\frac{w}{2} \right]$$

$$\text{For } i = 0, 1, \dots, \left[\frac{N}{\Delta u} \right], j = 0, 1, \dots, \left[\frac{M}{\Delta v} \right].$$

Figure 9a shows an image with some defects. The image size is 2592 × 1944; Δx and Δy are both 54 pixels. Δu and Δv which are 48 pixels and 36 pixels, respectively, can be derived from Equation 7. Figure 9b shows the corresponding Fourier domain image. The parameter w which is 10 is determined empirically. Hence, the generated mask is shown in Figure 9c. The filtered Fourier domain image is shown in Figure 9d. The restored image is shown in Figure 9e.

Defects classification

It can be observed from Figure 9e, that the restored image gives a significantly distinct gray value for the pixels belonging to the abnormal area, that is, defects. To separate the normal and abnormal area, the restored image was binarized under an empirically determined threshold t. The pixels which gray values are over t are abnormal area as shown in Figure 10.

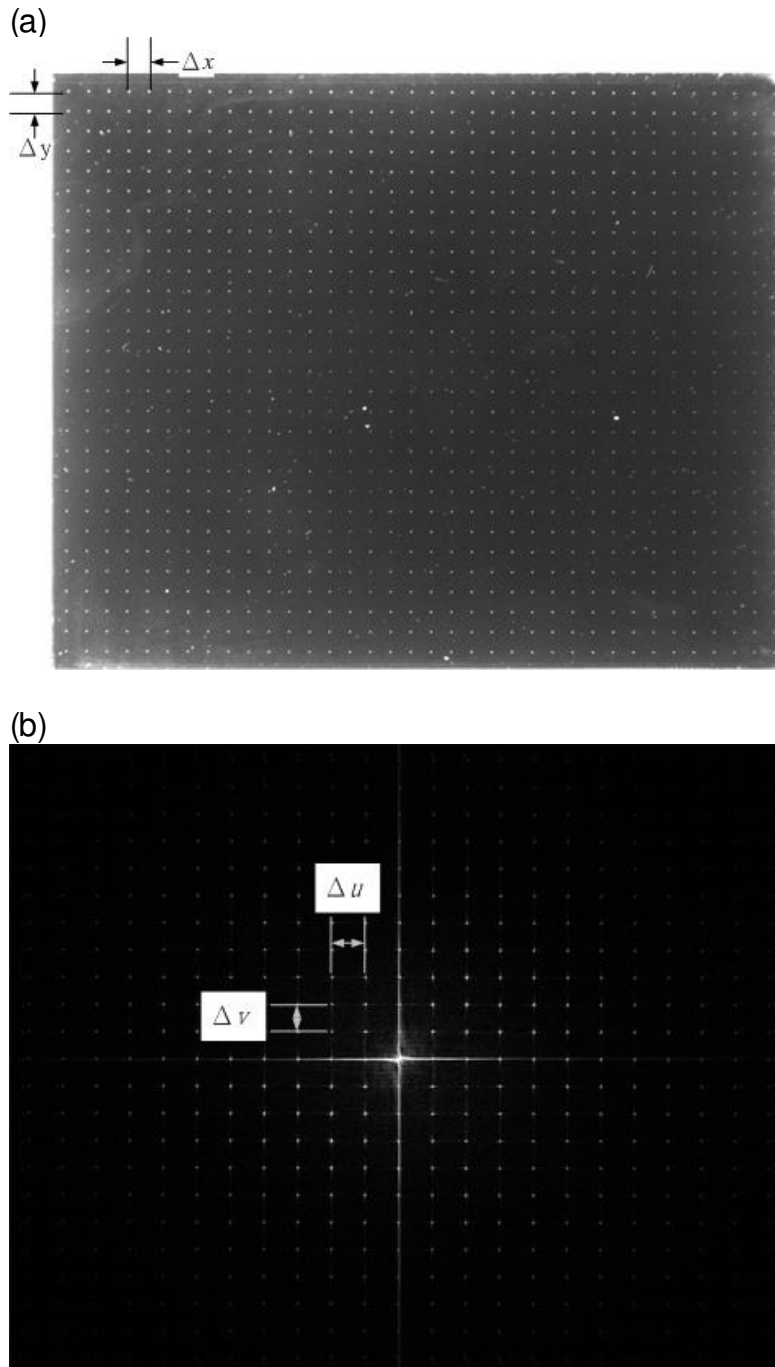


Figure 8. The touch panel image and corresponding Fourier spectrum.

The abnormal area can be classified as different kinds of defect, that is, scratch or spot, according to the shape features. First, the method of "Particle Measurements" (National Instrument Corp., 2007) was applied to group its pixels into defects and count the number of defects in the binarized restored image, as shown in Figure 11a. The morphological closing operation is adopted to connect the near defects as one defect as shown in Figure 11b.

Then two different shape features, such as area and roundness, were used to identify the kinds of defects. The definitions of the features of a blade are described as follows:

- Area: The number of pixels which belong to the defect.
- Roundness: If p is the center of the area, p_i the pixels and F the area of the contour. If the shape of defect is a circle, the value of roundness is equal to 1. The lower value of roundness means the shape of defect is more similar to the shape of line.

$$D = \sum_i \overline{pp_i} / F \quad (9)$$

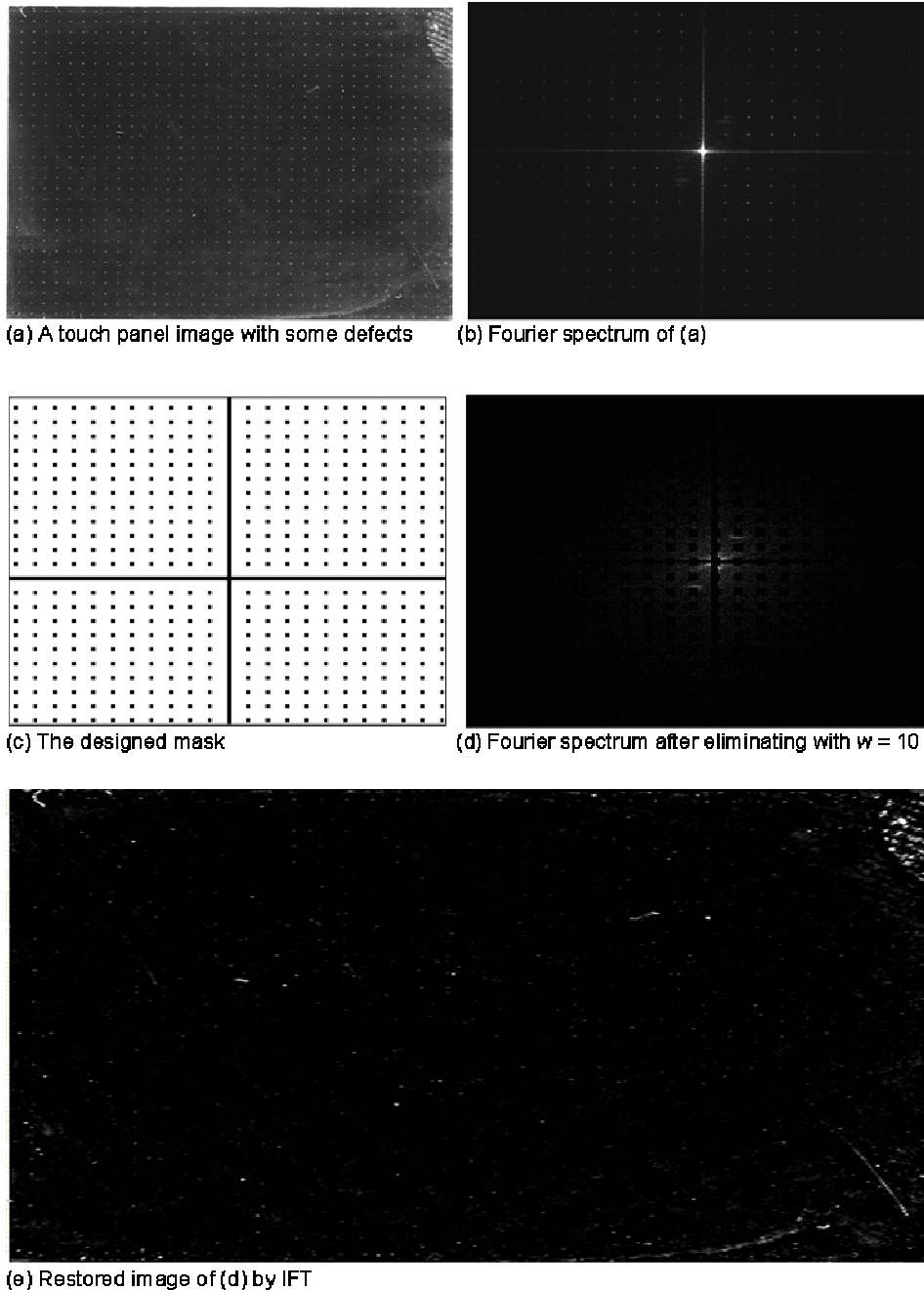


Figure 9. The image restoration procedure.

$$S = \sqrt{\sum_i (\overline{pp_i} - D)^2 / F}$$

$$\text{Roundness} = 1 - (S/F)$$

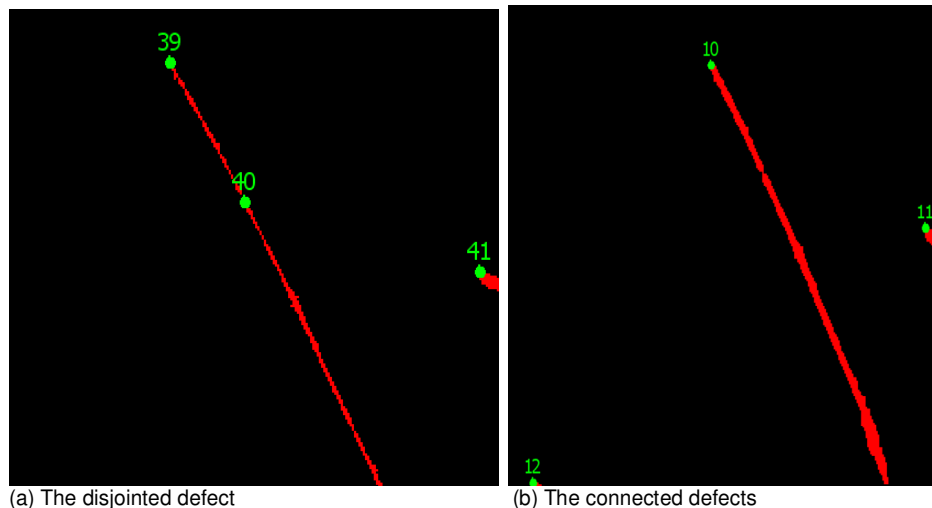
Two experimental parameters A_t and R_t which are determined empirically are used as threshold to classify the defects into three categories, Ignored noises, spot and linear foreign matter or scratch, as shown in Figure 6.

RESULTS

Here, we present the experimental results on several grabbed touch panel images to evaluate the performance of the proposed defect detected method. All the experiments are implemented on PC using LabVIEW of National Instruments and the prototype of the proposed AOI system. Each inspected image has 8-bit gray levels and 2592×1944 pixels. The inspection time for each touch panel is approximately 1 s.



Figure 10. The binarized image of the restored image.



(a) The disjointed defect

(b) The connected defects

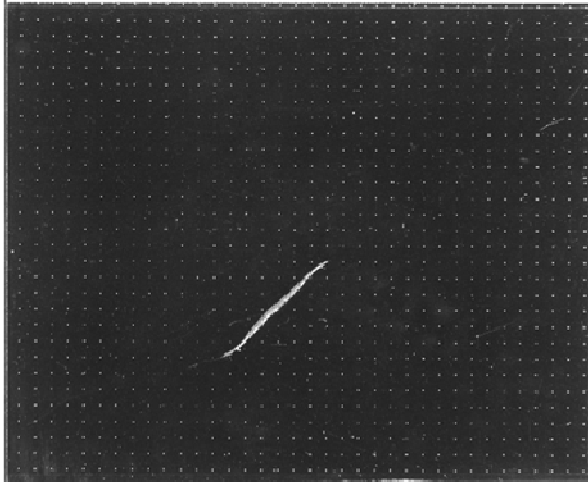
Figure 11. The result of connecting defect.

In the proposed method, there is a parameter w that may affect the inspection results. We had some experiments to evaluate the impact of varying of w on the effectiveness of defect inspection. Too large w may both remove the periodic regular structure and anomalies in the restored image, and may overlook subtle defects. However, too small w cannot completely remove all the periodic regular structure in the restored image and result in false alarms.

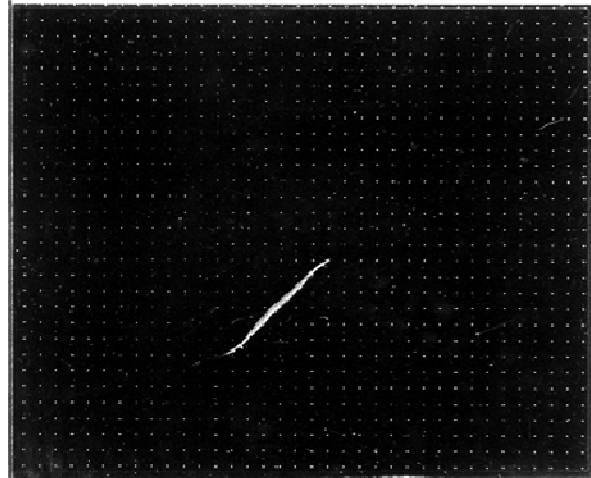
In the experiments, there a five different w values to be examined. The original image is shown in the Figure 12a. Figures 12b to f show the restored images with $w = 1, 3,$

$5, 10, 15$ pixels, respectively. It reveals that the restored image with small w , such as $w = 1, 3, 5$, cannot completely clean the periodic regular structure. A large w , such as $w = 10, 15$, can remove all the periodic regular structure in the restored image. However, too large w , such as $w = 15$, also remove partial anomalies in the restored image. Hence, all test images in the subsequent experiments use a fixed w of 10 pixels.

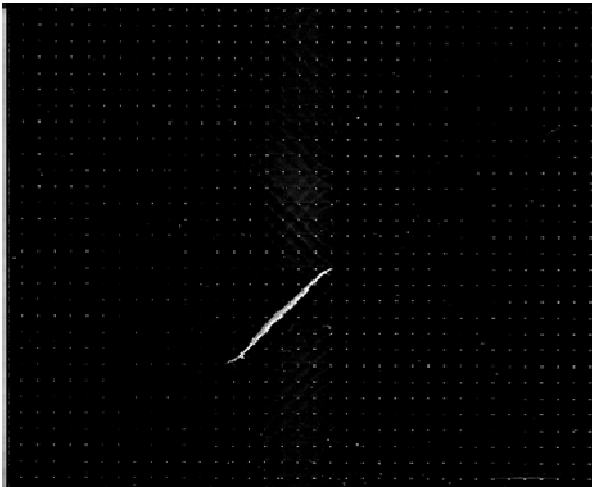
In this paper, the proposed defect detection method needs a parameter w to remove all the periodic regular structure. Then, we use an empirically determined threshold to separate normal and abnormal area. The



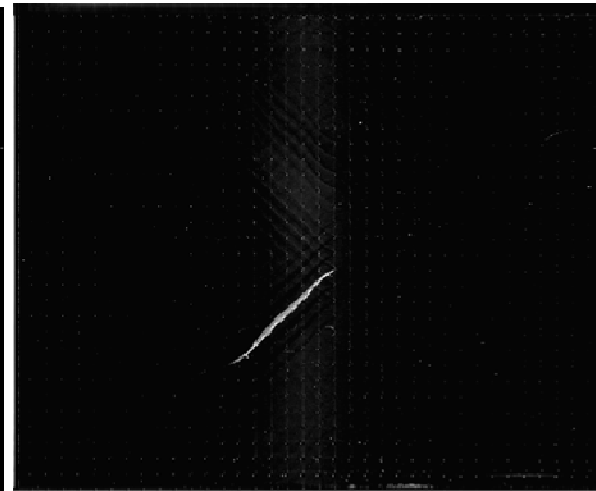
(a) Touch panel image



(b) Restored image of (a) with $w = 1$



(c) Restored image of (a) with $w = 3$



(d) Restored image of (a) with $w = 5$



(e) Restored image of (a) with $w = 10$



(f) Restored image of (a) with $w = 15$

Figure 12. The experimental results of parameter w .

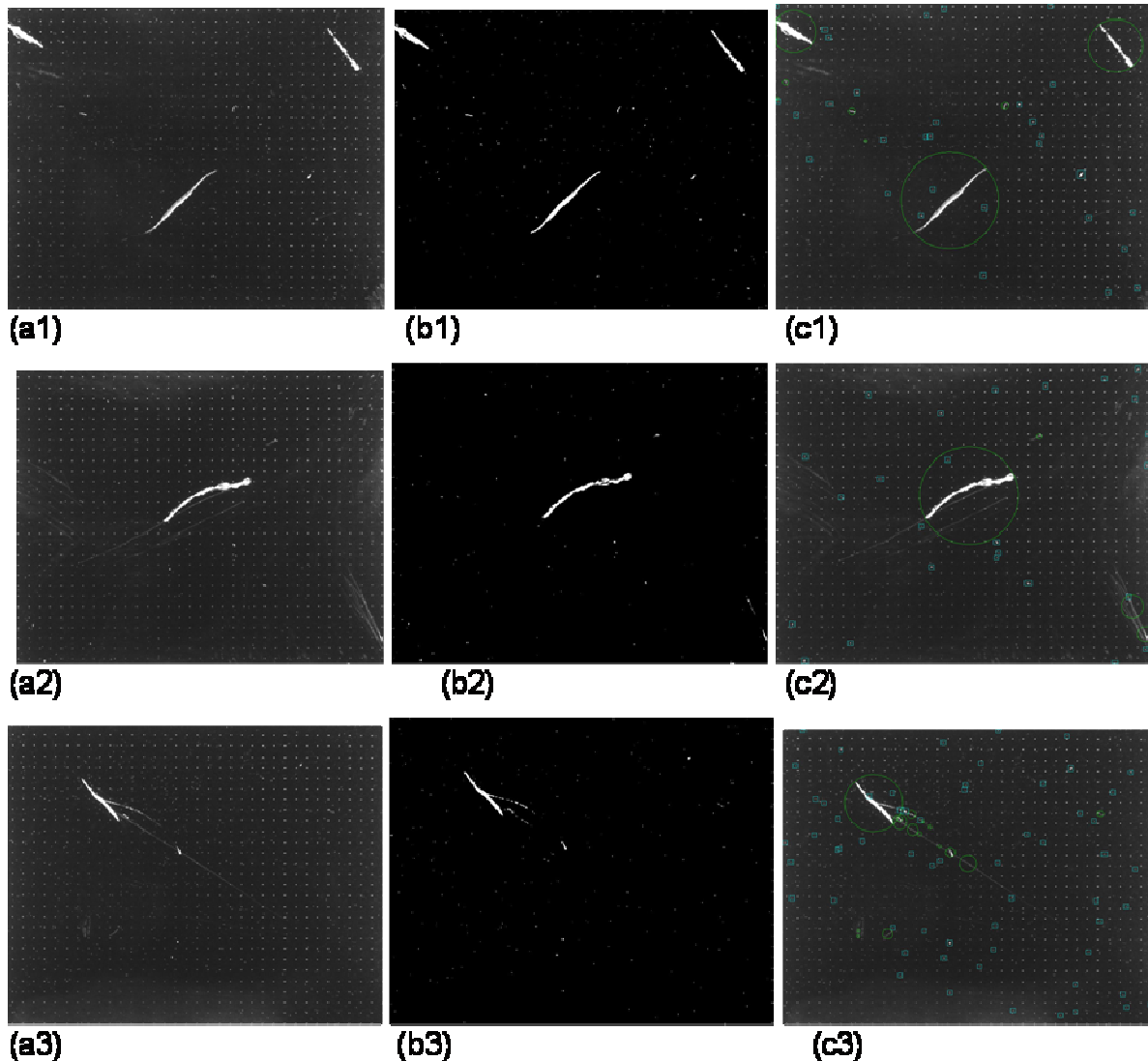


Figure 13. The inspected results of touch panel.

shape features, area and roundness, are used to classify the defects. Figure 13a1 to a3 shows three touch panel images. Figure 13b1 to b3 shows the corresponding restored images which is binarized by a threshold $t = 30$. All the periodic regular structure is removed and all the defects are preserved in the restored images. The results of defect detection and classification are shown in Figure 13c1 to c3. The scratch defect will be marked by a circle and the spot defect will be marked by a rectangle.

DISCUSSION

In the paper, we presented an AOI system that can identify the defect on the view-area of touch panel. Owing to the defects are inherently embedded in the periodic structure of the view-area, it is not easy to be inspected by human inspector. The proposed AOI system utilizes

the Fourier transform to remove the normal area (periodic structure) and preserve the abnormal area (defects). Otherwise, the proposed inspection method would also perform defect classification which is based on the shape features of the defect. The overall inspection cycle time of a touch panel with dimension 30×50 mm is around 1 s. The proposed AOI system can assist in determining the quality of touch panels. In future study, we aim to refine the inspection algorithm in order to solve the problems of image rotation and image distortion.

REFERENCES

- Chan CH, Pang G (2000). Fabric defect detection by Fourier analysis. *IEEE Trans. Ind. Appl.*, 36: 1267-1276.
- Chen SH, Perng DB (2011). Directional textures auto-inspection using principal component analysis. *Int. J. Adv. Manuf. Technol.*, 55(9-12): 1099-1110.

- Costa LD, Cesar RM (2000). Shape Analysis and Classification: Theory and Practice. pp. 421-464.
- Escofet J, Millan MS, Abril H, Torrecilla E (1998). Inspection of fabric resistance to abrasion by fouries analysis. Proc. SPIE 3490: 207-210.
- Gonzalez RC, Woods RE (2002). Digital image processing. Prentice Hall Second Edition, p.159.
- Kumar A (2008). Computer-vision-based fabric defect detection: A survey. IEEE Trans. Ind. Electron., 55(1): 348-363.
- Lin HD, Ho DC (2007). Detection of pinhole defects on chips and wafers using DCT enhancement in computer vision systems. Int. J. Adv. Manuf. Technol., 34(5-6): 567-583.
- Lu CJ, Tsai DM (2005). Automatic defect inspection for LCDs using singular value decomposition. Int. J. Adv. Manuf. Technol., 25: 53-61.
- Lu CJ, Tsai DM (2008). Independent component analysis-based defect detection in patterned liquid crystal display surfaces. Image Vis. Comput., 26: 955-970.
- National Instrument Corp. (2007). NI Vision Concepts Manual. National Instrument Corp., Austin, Texas, 10(1):10-19.
- Peng DB, Chen SH, Chang YS (2010). A novel internal thread defect auto-inspection system. Int. J. Adv. Manuf. Technol., 47(5-8): 731-743.
- Tsai DM, Chiang CH (2003). Automatic band selection for wavelet reconstruction in the application of defect detection. Image Vis. Comput., 21(5): 413-431.
- Tsai DM, Hsieh CY (1999). Automatic surface inspection for directional textures. Image Vis. Comput., 18(1): 49-62.
- UTECHZONE (2009). <http://www.utechzone.com.tw>